

MACROPHAGES EXPRESSING NEUROPILIN-1 AND BREAST TUMOR
PROGRESSION

by

Rachel Shannon Helms

A thesis submitted to the faculty of
The University of North Carolina at Charlotte
in partial fulfillment of the requirements
for the degree of Master of Science in
Biology

Charlotte

2015

Approved by:

Dr. Didier Dréau

Dr. Pinku Mukherjee

Dr. Jerry Troutman

©2015
Rachel Shannon Helms
ALL RIGHTS RESERVED

ABSTRACT

RACHEL SHANNON HELMS. Macrophages expressing neuropilin-1 and breast tumor progression. (Under the direction of DR. DIDIER DRÉAU).

Human breast carcinoma is the most commonly diagnosed cancer in women in the United States with patient mortality primarily resulting from metastasis of breast cancer cells to distant organs. Immune cells, including macrophages, are involved in cancer progression and their presence in primary breast tumors is a poor prognostic factor for patients. Therefore, in the present study we investigated the effects of macrophages in mammary tumor progression to elucidate critical intercellular interactions between these two cell types. Our results indicate that (1) co-implantation of 4T1 mammary tumor cells and RAW macrophages significantly decreased primary tumor mass but tended to increase metastases to the bone marrow. Also, (2) CD11b⁺ cell infiltration was higher in primary tumors derived from co-implantation of 4T1 and RAW cells. (3) Interestingly, apoptosis but not hypoxia was markedly increased in primary tumors generated from injection of 4T1 cells alone. (4) Consistent with the *in vivo* observations, in normoxic conditions co-culturing of 4T1 and RAW cells led to a reduction in the growth of 4T1 cells compared to 4T1 cells cultured alone. However, in similar co-cultures under hypoxic conditions, 4T1 cell growth was unaffected by the addition of RAW macrophages. (5) Additionally, regardless of oxygen conditions, in contrast with co-cultures using RAW macrophages, the addition of BMDMs to 4T1 cells did not alter the growth of the 4T1 cells. (6) Differential neuropilin-1 expression was observed between RAW macrophages and BMDMs. Taken together our data highlight the key role of oxygen conditions and macrophage phenotype in breast tumor progression.

ACKNOWLEDGEMENTS

First and foremost I would like to acknowledge my family for the continual support in all of my academic endeavors. They have always provided any assistance necessary along this rough road. Next, I would like to thank my mentor Dr. Didier Dréau. His guidance through the research process was continuously insightful and assisted me greatly in my research endeavors. The experiences I encountered within my time in his laboratory were indispensable to my development as an independent researcher.

I also would like to thank my committee members. Dr. Mukherjee's insight and in depth knowledge of tumor immunology was a great resource for my project. Meanwhile, Dr. Troutman continuously pushed me to do more and strive to improve each and every day.

Lastly, I would like to thank my lab family members who have assisted me along the way: Dr. Michelle Phelps, Dr. Stephen Rego, Amanda Patterson, Alex De Piante, and Bryanna Sierra.

TABLE OF CONTENTS

CHAPTER ONE: INTRODUCTION	1
CHAPTER TWO: MATERIALS AND METHODS	10
CHAPTER THREE: RESULTS	15
CHAPTER FOUR: DISCUSSION	25
CHAPTER FIVE: CONCLUSION	30
REFERENCES	33

CHAPTER ONE: BACKGROUND

Human breast carcinoma, with roughly 230,000 new cases each year in the US, is the most commonly diagnosed cancer in women [1]. Approximately 17 percent of these women will die due to the metastatic dissemination of cancer cells throughout their body [1]. Primarily seeding into the brain, liver, lungs and bones, metastatic breast cancer cells are responsible for patient mortality and treatment options for advanced stage patients are limited. Therefore, understanding the processes that govern the spread of cancer cells is critical in improving patient outcomes [2].

Significant evidence has implicated the evolution of a heterogeneous tumor microenvironment as a critical regulator in cancer progression [3, 4]. In addition to cancerous cells, the microenvironment contains various extracellular matrix (ECM) components and normal stromal cells, which include fibroblasts, adipocytes, endothelial cells, and leukocytes. Collectively, these micro-environmental factors can selectively promote or restrain tumor initiation and progression in a context specific manner [3-6].

The Microenvironment as a Regulator of Cancer

It has long been accepted that the tumor microenvironment can assist in tumor progression [7-9]. However, rediscovery of old evidence and new inquiries are demonstrating that the microenvironment can also effectively inhibit tumor progression

and is likely a determinant in cancer initiation [3, 10, 11]. The prevalence of undiagnosed *in situ* carcinoma, identified post-mortem in individuals with no known cancers, is indicative of the microenvironment's ability to constrain tumor progression [11]. Although whether these cancers would have progressed to malignancy is unknown, their incidence is often greater than the predicted likelihood of cancer development. For example, occult breast carcinomas were identified in 39% of 110 medico-legal autopsies, contrasting with the predicted 12% lifetime chance of developing breast cancer [1, 12]. Additionally, injection of cancerous mammary cells into normal stroma can lead to reversion of the cancerous phenotype and development of normal breast ductal and lobular structures, despite persistence of the genetic and epigenetic abnormalities within these cells [5, 13, 14]. Together these findings indicate a role for the tumor microenvironment in constraining tumor progression.

The ability of the microenvironment to assist in tumor initiation has been suggested by the finding that stromal breast density positively correlates with incidence of breast cancer development [15]. Additionally, stromal damage has been demonstrated to lead to epithelial cancer [16, 17]. To evaluate the role of the micro-environmental stroma in mammary tumor initiation, researchers have treated either stromal and/or mammary epithelial cells with a chemical carcinogen, *N*-nitrosomethyl urea (NMU). Specifically, the epithelial cells were removed from a rat mammary fat pad for treatment while the stroma was treated *in vivo*. The control and treated stroma and epithelial cells were then combined and implanted in the following 4 combinations: normal stroma/normal epithelia, exposed stroma/normal epithelia, normal stroma/exposed epithelia and exposed stroma/exposed epithelia. Interestingly, only animals that received

chemical carcinogen exposure to the stroma developed mammary tumors [17]. Moreover, the ability of the stroma to promote cancer initiation does not require carcinogenic exposure. Indeed, expression of matrix metalloproteinases (MMPs) by stromal cells can damage the basement membrane and lead to the development of mammary tumors [16].

In addition to facilitating initiation, the microenvironment is also capable of promoting cancer progression. This is evident as the survival of injected tumor cells subcutaneously is significantly increased when the cells are simultaneously injected with a tumor derived ECM or other stromal cell types [18, 19]. These micro-environmental components aid the tumor in developing independence from the host organ microenvironment while simultaneously altering the micro-environmental composition and structure so as to facilitate tumor progression and metastasis [5, 6]. Primarily this enhanced metastatic ability is facilitated by the angiogenic and inflammatory processes generated by the tumor microenvironment [9, 20-22].

Tumor Angiogenesis

As hypoxic areas begin to develop when the tumor diameter reaches about two millimeters (i.e., >300-1000 cells), the development of new vasculature from existing vessels is a critical component of breast cancer progression [23]. This angiogenic process is primarily assisted by the heterodimeric transcription factor hypoxia inducible factor -1 (HIF-1) in cancer cells [24]. The alpha subunit (HIF-1 α) is rapidly degraded in normoxia and accumulates in hypoxia while the beta subunit (HIF-1 β) is constitutively expressed [25]. Synthesized cytoplasmic HIF-1 α is immediately hydroxylated (P402, P564) and acetylated (K532) in an oxygen dependent reaction which favors association of HIF-1 α with the von Hippel-Lindau ubiquitin E3 ligase complex (pVHL) [26]. In turn, HIF-1 α is

rapidly degraded. When oxygen levels are low, however, the post-translational hydroxylation and acetylation reactions do not occur and HIF-1 α accumulates within the cytoplasm where it can then readily dimerize with HIF-1 β , an aryl hydrocarbon receptor nuclear translocator (ARNT) [24, 26]. Subsequently, the dimer translocates to the nucleus where it regulates transcription of hypoxia related genes, including Vascular Endothelial Growth Factor (VEGF) [24].

Within the breast tumor microenvironment the expression of HIF-1 α is correlated with increased pathologic stage [24]. Additionally, as HIF-1 α expression increases, VEGF expression and endothelial cell microvessel density increase [24]. These findings indicate the hypoxic tumor microenvironment aids in the development of vascularization of the tumor. This is critical in cancer progression as the new vessels provide nutrients to the primary tumor, remove waste and act as routes leading away from the tumor for metastasis [27].

VEGF Signaling

VEGF is a potent dimeric glycoprotein that is known to facilitate angiogenesis *in vivo* [28]. Particularly, VEGF promotion of angiogenesis is achieved through its binding to VEGF receptor 2 (VEGFR2) leading to trans-auto-phosphorylation of the receptor tyrosine kinase and downstream signaling that enhances survival, proliferation, and migration of the cell expressing the receptor [28]. This signaling is further enhanced when Neuropilin-1 (NRP-1), a co-receptor, is expressed. Specifically, NRP-1 acts as a co-receptor for the predominantly secreted VEGF isoform 165 [29]. Although the cytoplasmic tail of NRP-1 is not currently known to transduce signals, the extracellular binding domains of NRP-1 can bind VEGF 165 [30]. The resulting VEGFR2-VEGF-

NRP-1 complex (Figure 1, adapted from [29]) significantly improves the binding affinity of VEGF to VEGFR2 enhancing cellular migration to the VEGF stimuli [28, 31].

Accordingly, survival and proliferation signals are enhanced within these cells [29].

Interestingly, NRP-1 can also act as a co-receptor VEGF 165 with VEGFR1; however, this interaction has predominately been detailed as a VEGF 165 decoy interaction and directly inhibits angiogenesis [32].

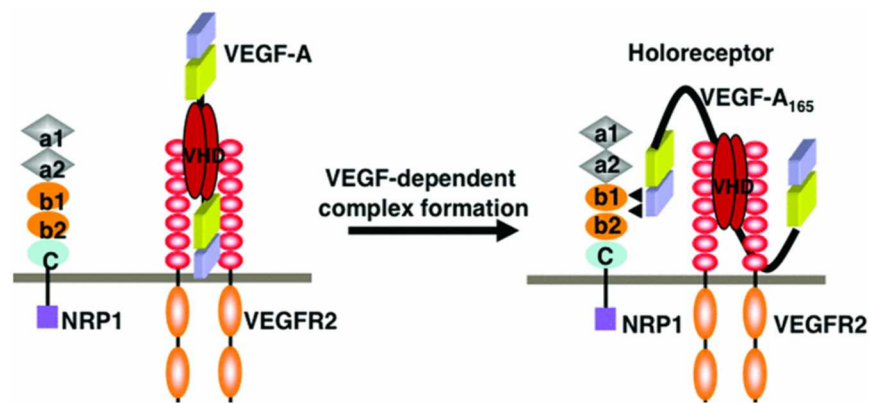


Figure 1: VEGFR2-VEGF-NRP-1 Complex. VEGF binds VEGFR2 at the second and third extracellular immunoglobulin domains while simultaneously binding NRP-1 through its B (b1, b2) domain. Adapted from Zachary, I.C. 2011.

Neuropilin-1

In addition to VEGF, NRP-1 is also a known co-receptor for semaphorin 3A (SEMA 3A), a secreted protein capable of acting as both a chemoattractive and chemorepulsive stimuli [33]. Specifically, SEMA3A utilizes NRP-1 as a co-receptor in binding to class A plexins [33]. Indeed, binding of SEMA3A, A-type plexins, and NRP-1 results in complex formation leading to enhanced migration to the SEMA3A source. This is achieved by type-A plexin receptor dimerization and activation leading to changes in integrin-mediated cell adhesion as well as cytoskeletal structural rearrangement [34]. The ability of NRP-1 to mediate migration and therefore localization of cell types via

enhancing SEMA3A and plexin signaling was first identified in neuronal and cardiovascular systems [34]. Accordingly, subsequent research has evaluated the ability of this interaction to facilitate immune cell trafficking [35, 36]. SEMA3A complex formation has been found to be important in trafficking of myeloid immune cells (most notably macrophages and dendritic cells) [37-39].

Additionally, given the importance of vascularization within the tumor mass [40] and the clear role NRP-1 has in recruiting mediators in angiogenesis, the expression and role of NRP-1 in tumor progression has been evaluated. Expression of NRP-1 has been shown to be upregulated within cancer, and even correlates with tumor progression [41]. Enhanced NRP-1 expression within the tumor microenvironment can promote tumor progression through multiple mechanisms. Endothelial cells expressing NRP-1 directly enhance angiogenesis, while tumor cells expressing NRP-1 can more potently respond to proliferative signals (i.e., VEGF), and demonstrate increased migratory and metastatic potential [41-43].

Inflammation

In addition to angiogenesis, chronic micro-environmental inflammation has been recognized as a major contributor to tumor progression [20]. Early in tumorigenesis, lymphocytes are capable of recognizing and eliminating tumor cells through acute inflammatory responses in a process known as immuno-surveillance [20, 44]. Specifically, T helper lymphocytes (Th) are phenotypically skewed to a Th1 response in which they secrete interferon-gamma (IFN- γ) capable of arresting the cell cycle and promoting apoptosis in tumor cells expressing the IFN- γ receptor [45]. Additionally, cytotoxic T lymphocytes (CTLs) expressing granzyme B and perforins induce apoptosis

of target cancer cells. Together these interactions can result in elimination of the tumor mass or in the development of an equilibrium between the growth and destruction of tumor cells [44]. However, as the normal microenvironment is disrupted and the tumor microenvironment expands, the processes favoring immune recognition and elimination of cancer cells become less efficient [46]. Accordingly, the micro-environmental signals change resulting in an altered phenotype and functionality of immune cells leading to a chronic inflammation within the tumor [20]. For example, the Th cell population skews to a Th2 response which secretes cytokines that promote T cell anergy and loss of CTL activity [47], and regulatory immune cells are recruited to the tumor microenvironment to further enhance immune suppression (Figure 2, adapted from [20]).

In addition to lymphocytes, other immune cell types, including macrophages, are present in the inflammatory microenvironment [48]. As an extremely plastic innate cell type, macrophages can differentiate along a spectrum of possible phenotypes with the extremes being recognized as classically (M1) and alternatively activated (M2) [49]. Within the tumor microenvironment, M1 macrophages are typically associated with acute inflammation and fulfill anti-tumor functions [49]. In contrast, M2 macrophages directly and indirectly mediate pro-tumor functions that assist in tumor growth and metastasis [48, 50, 51]. Specifically, tumor associated macrophages (TAMs) enhance breast tumor progression through repressing the adaptive immune response, promoting vascularization of the primary tumor, and stimulating tumor cell invasion and metastasis [48, 50-53]. Accordingly, infiltration of macrophages into the tumor microenvironment is associated with decreased patient survival particularly when the ratio of M2:M1 macrophages is high [53, 54].

Hypoxia is a major contributor to the M2 TAM phenotype [55-57]. The remarkable phenotypic and metabolic plasticity associated with macrophages, allows TAMs to enter into hypoxic tumor areas, activate HIF-1 α , and subsequently upregulate M2 markers [55]. Macrophages exposed to hypoxia increase their expression of the M2 cell surface markers CD163 and CD206 [57]. Moreover, they secrete elevated levels of VEGF as well as MMP-2 and MMP-9 [56]. These molecules lead to increased angiogenesis and matrix remodeling which enhance tumor progression [55, 57]. Additionally, hypoxia increases TAM expression of IL-10 and TGF- β , which in turn suppress CTL activity and skew Th cells toward a Th2 phenotype [58-61].

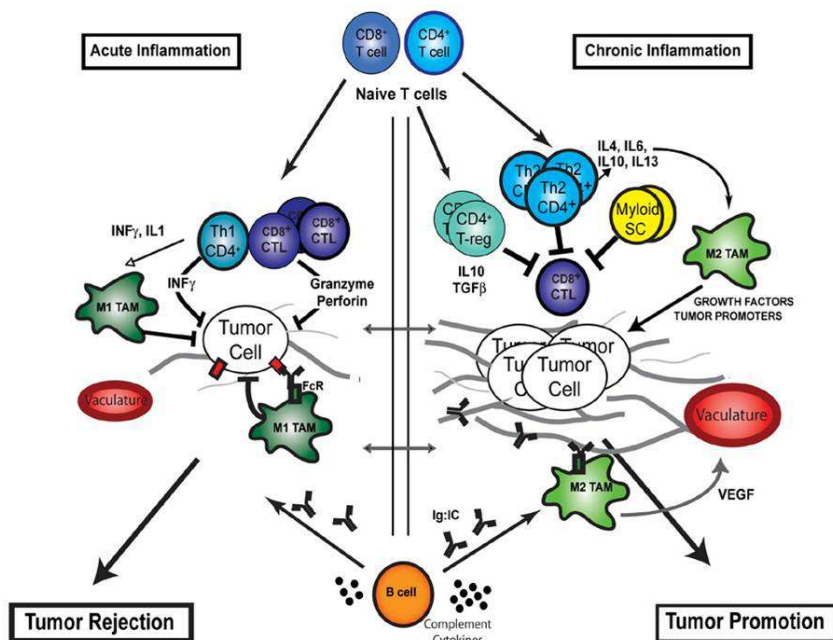


Figure 2: Inflammatory responses within the tumor microenvironment. A cute inflammation (left) favors M1 macrophages, Th1 Cd4+, and CD8+ T cytotoxic lymphocyte populations leading to tumor rejection. Chronic inflammation (right) favors M2 macrophages, Th2 CD4 +, and T-regulatory cells to promote tumor progression. Adapted from Denardo, D.G, et al, 2007.

As M2 macrophage infiltration into breast tumors is a poor prognostic factor for patients and the exact mechanisms by which M2 macrophages are recruited and maintained within the tumor microenvironment are unclear, our lab has focused on studying interactions between tumor cells and macrophages to elucidate critical intercellular interactions that facilitate pro-tumor macrophage functions [62, 63]. Recently our lab has evaluated the effects of orthotopic co-injections of murine macrophages (RAW) with murine metastatic mammary carcinoma cells expressing red fluorescent protein (4T1-RFP). Unexpectedly, the co-administration of RAW macrophages and 4T1 tumor cells significantly decreased tumor size compared to injection of 4T1 alone contrasting with one previous study in which co-implantation of 4T1 and M2 activated bone marrow derived macrophages (BMDMs) led to increases in tumor size [64]. Thus, the present study further evaluates the hypothesis that 4T1 tumor growth is altered by immune cells present in the microenvironment.

CHAPTER TWO: MATERIALS AND METHODS

Cell Origin and Culture

Murine metastatic mammary carcinoma cells (4T1), endothelial cells (2H11) and macrophages (RAW 264.7, hereto forth abbreviated as RAW) were purchased from American Type Culture Collection (ATCC, Manassas, VA). Media and supplements were obtained from Hyclone (Logan, UT) unless noted. 4T1, 2H11 and RAW cells were cultured at 37°C and 5% CO₂ in a 2:1 ratio of RPMI and DMEM F-12, respectively. This media was supplemented with 10% fetal bovine serum (FBS; Atlanta Biologics, Atlanta, GA), 0.1 % gentamycin, and 1.0 % amphotericin B. Bone marrow derived macrophages (BMDMs) were derived from the bone marrow of C57BL/6 mice as described previously [65]. Briefly, bone marrow was flushed from the femurs and tibias of four mice and seeded into two 75 mm² Corning Flasks. After attachment, the media was removed and replaced with RPMI:DMEM/F-12 (2:1) supplemented with 50 ng/ml macrophage colony stimulating factor (M-CSF) to induce macrophage differentiation. This media was changed every three days for two weeks.

In Vivo Experiment

Female Balb/C mice (Jackson Lab, Bar Harbor, ME) were housed and maintained in the Vivarium in accordance with the guidelines of the Institutional Animal Care and Use Committee of the University of North Carolina at Charlotte. Mice were injected

subcutaneously in the second left inguinal mammary fat pad with 3×10^5 RFP-expressing 4T1 cancer cells (Anticancer Inc., San Diego, CA) in 100 μ l of PBS. Cancer cells were either injected alone, or with RAW macrophages (ratio: 5 cancer cells to 1 macrophage). Tumor growth was assessed by caliper measurements and tumor volume derived (mm^3) [66] and by fluorescence, measured as fluorescent radiant efficiency ($[\text{p/s/cm}^2/\text{sr}]/[\mu\text{W/cm}^2]$), over a 28-day period using an in vivo imaging system (IVIS, Perkin Elmer, Waltham, MA).

Flow Cytometry for Bone Marrow Metastasis

Following animal euthanasia, bone marrow suspensions were obtained from mice injected with 4T1-RFP cells alone ($n=4$) or co-implanted with 4T1-RFP cells and RAW cells ($n=4$) were prepared. Briefly, the bone marrow was flushed from the femurs and tibiae and fixed in 2 % para-formaldehyde for 15 minutes. Subsequently, 15 μ L of the cell solutions were stained for nuclei with 400 μ L of Hoechst (1:2000) in phosphate buffered saline (PBS). After one hour, the samples were run using a flow-cytometer (Fortessa, BD Biosciences, San Jose, CA). RFP positive 4T1 cells in the bone marrow were identified as the percent of DAPI/RFP double positive cells.

Immune Cell Subsets in Primary Tumors

Primary tumors were collected at euthanasia with half of the tumor fixed for immuno-histochemical analyses and half used to generate a cell suspension. Briefly, half of the tumor was minced and passed through a cell strainer (BD, Biosciences). The obtained cell suspensions were fixed in 2% para-formaldehyde and stored at 4°C until use.

Immune subsets CD8 (cat#BD553031 – FITC Rat anti-mouse; BD Biosciences), CD4 (Cat#60029AZ.1 – APC – Rat anti-mouse; Stem Cell Technologies), and CD11b (Cat#BD552850 – PE-Cy7 Rat anti-mouse; BD Biosciences) were assessed in tumor suspensions. Briefly, after a blocking step (12.5% BSA), tumor suspensions (50 μ L) were incubated with conjugated primary antibodies or isotype controls (dilution: 1:100 6.25% in blocking solution). After two washes, percentages of CD8+, CD4+ T cells were identified as FITC/DAPI and APC/DAPI double positive cells, respectively. The percent of myeloid cells (CD11b+) were identified as the PE-Cy7/DAPI double positive cells.

Macrophage Subsets

Macrophages present in the bone marrow and primary tumor suspensions i.e., BMDM, obtained from the in vivo murine experiment (see details above) and RAW cells from in vitro cultures were assessed for NRP-1 expression by flow-cytometry. Briefly, after a fixation step, cells were permeabilized in 100 % cold methanol for 15 minutes on ice. Next, cells were blocked in 12.5 % bovine serum albumin (BSA) with the nuclear dye Hoechst (1:2000) diluted in PBS. Primary, secondary, and control antibodies were diluted in 6.25% BSA. NRP-1 expression on cells was determined using a rabbit anti-mouse anti-neuropilin 1 antibody (Ab81321, Abcam, CA; dilution, 1:100). After washing with PBS, an APC conjugated anti-rabbit secondary antibody (BD Biosciences; dilution, 1:500) was used to detect the rabbit anti-neuropilin. NRP-1 positive cells were identified as APC/DAPI double positive cells. Additionally, the APC mean fluorescence intensity (MFI) an indication of the intensity of the stain associated with the density of neuropilin-1 expression was recorded.

Immunohistochemistry

Primary tumors (half, see above) collected at euthanasia were fixed in formalin, paraffin-embedded and sections (5-7 um section thick) were attached onto slides. Immunohistochemistry analyses to assess apoptosis, hypoxia, and inflammation were conducted. Briefly, slides were incubated for 30 min in 62°C to melt the paraffin and slides were then transferred from xylene, 100 % ethanol, 95% EtOH, 70% EtOH, and to water to remove the paraffin and rehydrate the tissue. Antigen retrieval was conducted using antigen retrieval solution (Dako) for 25 minutes in a steamer. Following a cool-down period, and rinses with water, slides were incubated in hydrogen peroxide (1%) in methanol to quench the intrinsic peroxidase activity and then blocked with 50% FBS for 60 minutes. Next, slides were incubated with either the primary antibody or incubating buffer (15% FBS) (i.e., each slide included at least 2 tumor tissue cuts) for 3 hours in an humidified chamber at RT. Slides were then washed twice in PBS and incubated with the appropriate species biotin-conjugated secondary antibody (Jackson immunoResearch Laboratory) diluted in incubation buffer for 30 min. at RT. Following washes, incubation with Streptavidin-HRP (Vectastain Universal horseradish peroxidase system; Vector Laboratory, Burlingame, CA), the detection of the protein of interest was carried out using diaminobenzidine (DAB, Vector lab.). Slides were next rinsed in water and counterstained with Hematoxylin (Hematoxylin QS, Vector lab.). Tissues were then dehydrated in increasing concentrations of ethanol and slides were mounted in a non-aqueous mounting agent (Vector lab). Light microphotographs were taken at 200X on an IX71 microscope fitted with a DP70 camera (Olympus). Staining and expression of

specific antigens including active caspase 3, HIF1 α , and CD45 were assessed using Cell Profiler software (<http://cellprofiler.org/>) accounting for the intensity of the stain.

In Vitro Tumor Cell - Macrophage Co-cultures

4T1-RFP expressing mammary carcinoma cells (100,000 cells) and RAW macrophages (20,000 cells) were seeded either alone or together in 1.5 mL of 10 % FBS RPMI:DMEM/F-12 media in 12 well plates. These cells were then either cultured in normoxia (21% O₂) or in a hypoxic chamber (MIC-101: Billups-Rothenberg, Inc., Del Mar, CA), which was flooded with N₂ gas for two minutes then sealed, for 48 hours (<1% O₂). Following incubation, cells were stained with Hoechst (1:2000) for one hour and the fluorescence for the nuclei (360/460, sensitivity=50) and RFP (530/590, sensitivity = 50) were recorded using a fluorescent plate reader (BioTek Synergy HT, Winooski, VT). The abundance of RFP positive 4T1 cells was expressed as the ratio of RFP/Hoechst. Additionally, representative microphotographs were taken using an IX71 fluorescent microscope (Olympus, Center Valley, PA) equipped with a DP70 camera (Olympus). For each condition, microphotographs were quantified for the intensity of RFP and the number of nuclei using Cell Profiler software.

Statistics

All data are presented as means \pm standard error of the mean (SEM) unless noted. Statistical significance was determined using Prism software (Graphpad Software, Inc., La Jolla, CA). Experiments were analyzed using t-tests (two groups) or one-way ANOVA followed by Tukey's post-hoc test (3 or more groups, one factor). Data with a non-normal distribution was normalized using a log transformation as indicated. Significance was set *a priori* to p value below 0.05.

CHAPTER THREE: RESULTS

1- In vivo, co-implantation of RAW and 4T1 led to a decrease in primary tumor growth

In vivo the co-administration of 4T1-RFP cells with RAW macrophages was associated with a significantly slower growth of the primary tumor as determined by fluorescence intensity and caliper measurements over time ($p < 0.001$, ANOVA repeated measures, Figure 3).

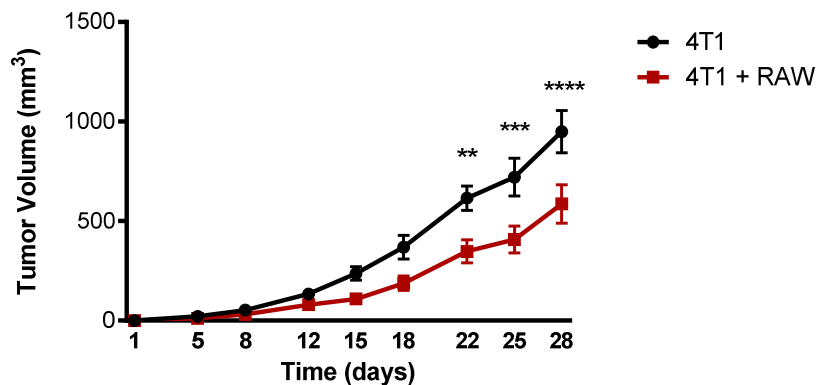


Figure 3: Growth of 4T1-RFP mammary carcinoma cells in BALB/c mice. A Tumor volume (mm³) over time. All data points represented as mean +/- SEM. ** $p < 0.01$, *** $p < 0.001$, **** $p < 0.0001$. $n = 8$.

2 - Variation of immune populations within the primary tumors following co-administration of 4T1-RFP and RAW cells

The infiltration of immune cells into the tumor microenvironment was assessed in primary tumors isolated from mice implanted with 4T1-RFP cells alone and 4T1-RFP

cells with RAW macrophages. CD45⁺ hematopoietic cells were identified by immunohistochemical analysis of tumor tissues. No significant difference was observed in CD45 expression within the co-injected and 4T1-RFP alone tumor sections ($p = 0.1582$, $n = 8$, Figure 4).

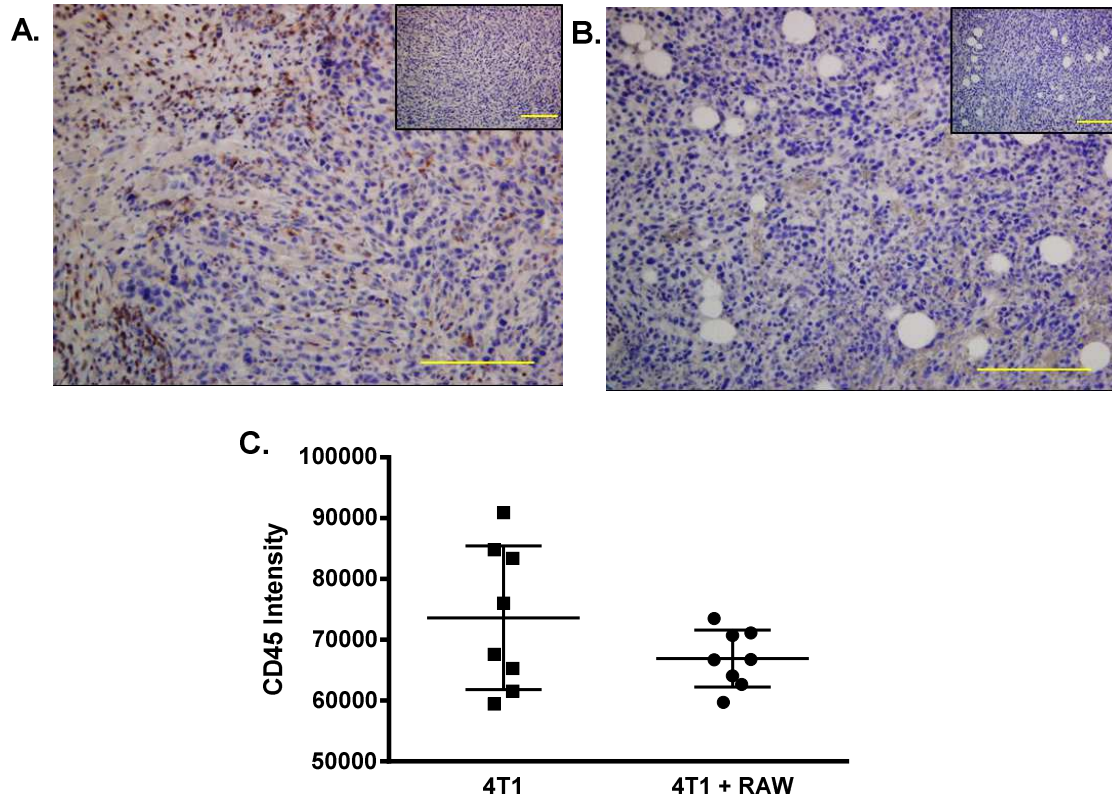


Figure 3: IHC analysis of CD45 expression in 4T1-RFP mammary tumor sections derived from implantation of 4T1-RFP alone (A) or 4T1-RFP and RAW (B). (C). Quantification ($n=8$) of CD45 IHC staining. Scale bar = 200 μm . Inset images are control tumor sections stained with secondary antibody only.

Percentages of CD4⁺ T helper, CD8⁺ T cytotoxic lymphocytes, and CD11b⁺ immune cells were determined in tumor cell suspensions using flow cytometry. There was no significant difference observed in the percent of CD4 ($p = 0.3954$, $n = 4$, Figure 5A) or CD8 ($p = 0.2481$, $n = 4$ Figure 5B) positive cells between the two tumor groups.

Although no differences were observed in the percentages of CD4 and CD8 positive T cells present within the primary tumor mass, the functionality of these cell types within the two different tumor groups may differ drastically [39].

However, a significant increase in the percent of CD11b+ cells within primary tumors of mice implanted with 4T1-RFP and RAW cells compared to those injected with 4T1 cells alone was observed ($p = 0.0306$, $n = 4$ Figure 5C). CD11b is expressed on myeloid precursor cells in low levels and is increased in mature monocytes, macrophages and neutrophils [67]

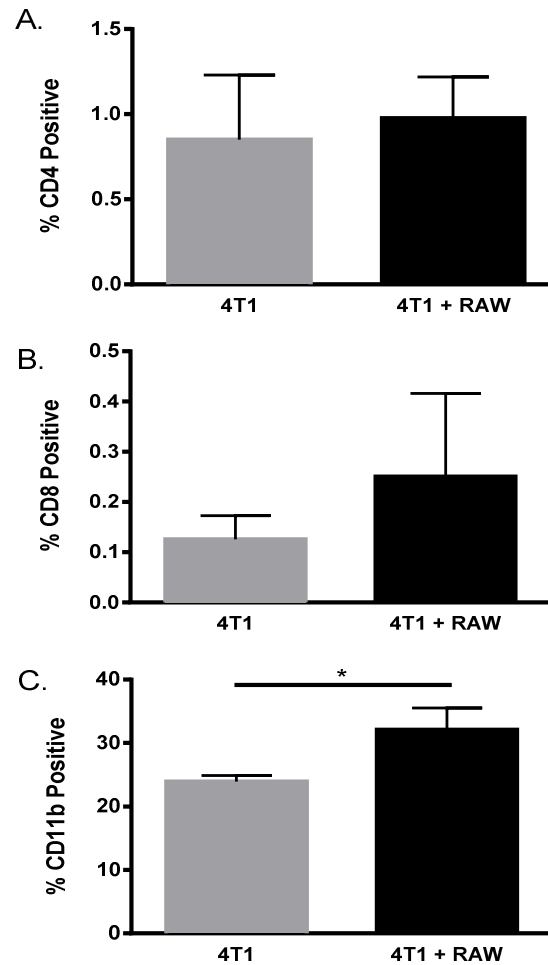


Figure 5: Immune infiltration of 4T1-RFP orthotopic tumors in BALB/c mice. Infiltration of CD4+ (A), CD8+ (B), and CD11b+ (C) cells at day 28. Data points are represented as the mean \pm SEM. $n = 4$. * $p < 0.05$.

3- Apoptosis decreased significantly in the primary tumor following the co-administration of RAW cells with 4T1 cells

Given the increased number of CD11b⁺ cells in tumors derived from animals co-implanted with 4T1 and RAW cells and the associated decrease in tumor growth, we next investigated apoptosis through the expression of active caspase-3 by IHC in primary tumors. A critical effector of apoptosis, caspase-3 is synthesized as an inactive proenzyme that upon activation of apoptotic cascades is cleaved into active fragments [68]. A significant decrease in active caspase-3 in the primary tumors from mice co-implanted with 4T1-RFP and RAW cells compared to mice injected with 4T1 cells alone was detected ($p = 0.008$, $n = 8$, Figure 6).

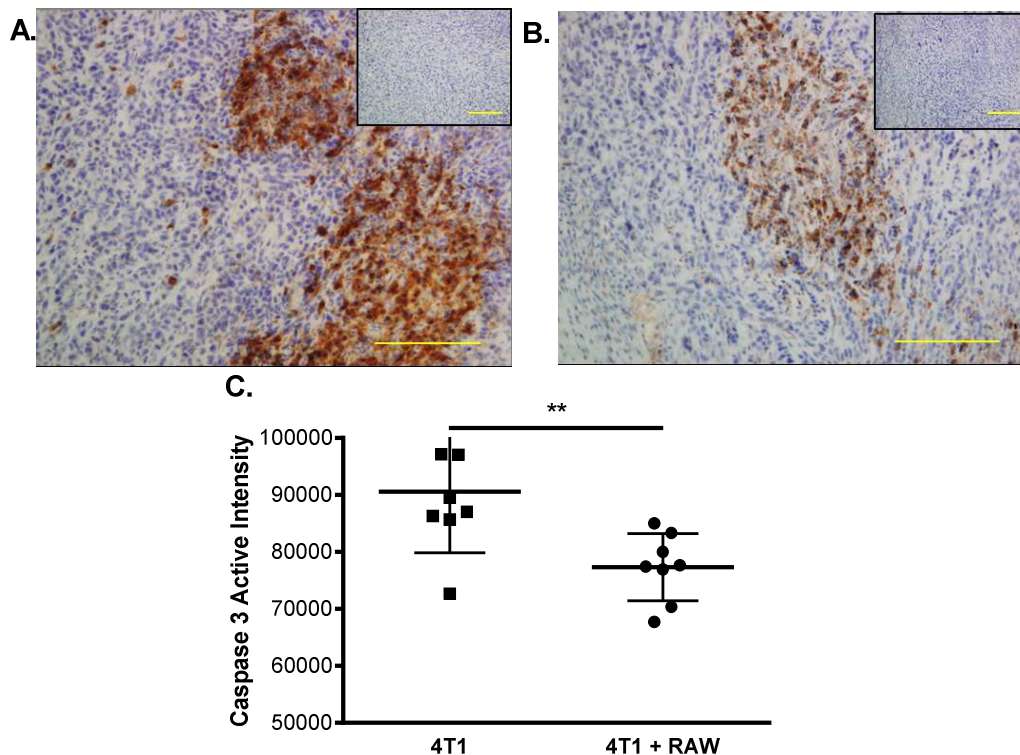


Figure 6: Expression of Caspase 3 active in 4T1-RFP orthotopic tumors in BALB/c mice. Representative microphotographs of 4T1-RFP (A) and 4T1 + RAW (B) tumors. (C) Quantification of IHC microphotographs. Data points are represented as the mean \pm SEM. $n = 8$. * $p < 0.05$. Scale bar = 200 μ m. Inset images are control tumor sections stained with secondary antibody only. as mean \pm SEM. ** $p < 0.01$.

4 – HIF1 α expression in primary tumors following the administration of 4T1 cells alone or the co-administration of RAW and 4T1 cells

The ability of the implanted RAW cells and recruited CD11b⁺ cells to assist in tumor regression is dependent on their ability to maintain an anti-tumor phenotype [48, 50, 69]. As pro-tumor phenotypes are promoted by hypoxia within the tumor microenvironment, we next evaluated HIF-1 α expression by IHC. No significant difference in the intensity of HIF-1 α expression within the two tumor groups was detected by IHC ($p = 0.5935$, $n = 8$, Figure 7).

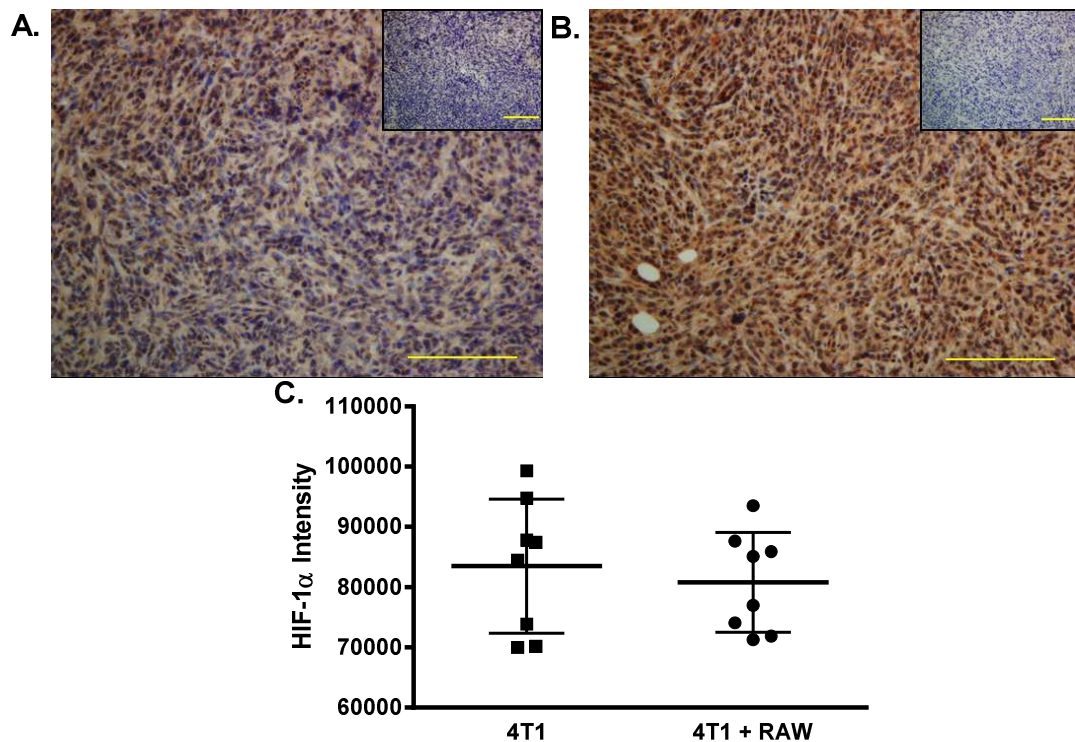


Figure 7: Expression of HIF - 1 α in 4T1-RFP orthotopic tumors in BALB/c mice. Representative microphotographs of 4T1-RFP (A) and 4T1 + RAW (B) tumors. (C) Quantification of IHC microphotographs. Data points are represented as the mean \pm SEM. $n = 8$. * $p < 0.05$. Scale bar = 200 μ m. Inset images are control tumor sections stained with secondary antibody only.as mean \pm SEM.

5 – The key determinant of macrophage phenotype, Neuropilin-1, is differentially expressed

Previously, neuropilin-1 (NRP-1) has been shown to be a crucial determinant in macrophage phenotype through localizing macrophages to hypoxic tumor regions [39]. Furthermore, knocking down NRP-1 expression prevents macrophage localization to hypoxic tumor areas and promotes/maintains the M1 phenotype [5]. This macrophage phenotype supports a significantly higher recruitment of macrophages to the tumor site, and significant decreases in tumor volume and metastases [39]. Thus, we hypothesized the RAW macrophages co-injected with the 4T1-RFP cells had a decreased expression of NRP-1 resulting in their maintenance of an anti-tumor phenotype. NRP-1 expression was evaluated by flow cytometry on bone marrow derived macrophages (BMDM), RAW cells and 2H11 endothelial cells (positive control).

Although no significant difference was observed in the percent of NRP-1 positive cells between the 3 cell types tested ($p = 0.1352$, (RAW, $n=9$), (BMDM, $n=2$), (2H11, $n=10$), Figure 8A), a significant difference in the NRP-1 mean fluorescence intensity (MFI; $p = 0.0101$, (RAW, $n=7$), (BMDM, $n=2$), (2H11, $n=10$), Figure 8B) was observed. In particular, the RAW cell MFI was significantly lower than that of 2H11 endothelial cells ($p < 0.01$). Also, the RAW cell MFI tended to be lower than that of the BMDM cells ($p = 0.0582$, t-test).

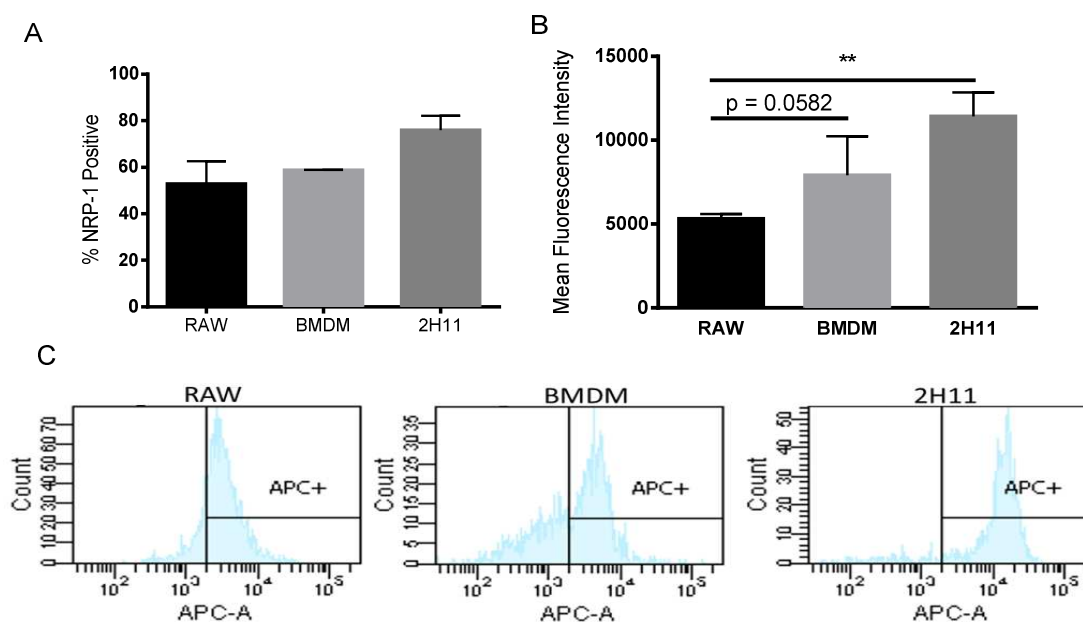


Figure 8. Expression of NRP-1 by RAW, BMDM, and 2H11. A. There is no difference in the percent of NRP-1 positive cells. B. There is a significant difference in RAW and 2H11 mean fluorescence intensity when stained for NRP-1. C. Representative histograms of NRP-1 mean fluorescence intensity quantified in B. Data points are represented as the mean \pm SEM. ** $p < 0.01$

6 – Metastatic burden following co-administration of 4T1-RFP and RAW cells

Decreased macrophage expression of NRP-1 has been associated with both decreased primary tumor volume and metastases [39]. Thus, we evaluated the metastatic burden of the 4T1-RFP carcinoma cells to the bone, liver, lungs, and spleen using the IVIS system. No significant difference in metastatic tumor burden between mice co-injected with 4T1 and RAW cells and mice injected with 4T1-RFP alone was observed ($p = 0.3933$, $n = 8$, Figure 9A). However, metastasis to the bone was significantly higher, regardless of the animal group compared to other sites ($p < 0.0001$, $n = 8$). Thus, we further evaluated metastases to the bone, by assessing the percent of 4T1-RFP⁺ cells within the bone marrow cell suspensions. Interestingly, bone marrow suspensions derived from animals co-injected with RAW and 4T1-RFP tumor cells tended to have increased

numbers of 4T1 cells compared bone marrow suspensions obtained from mice injected with 4T1 cells alone ($p = 0.0689$, $n = 4$ Figure 9B).

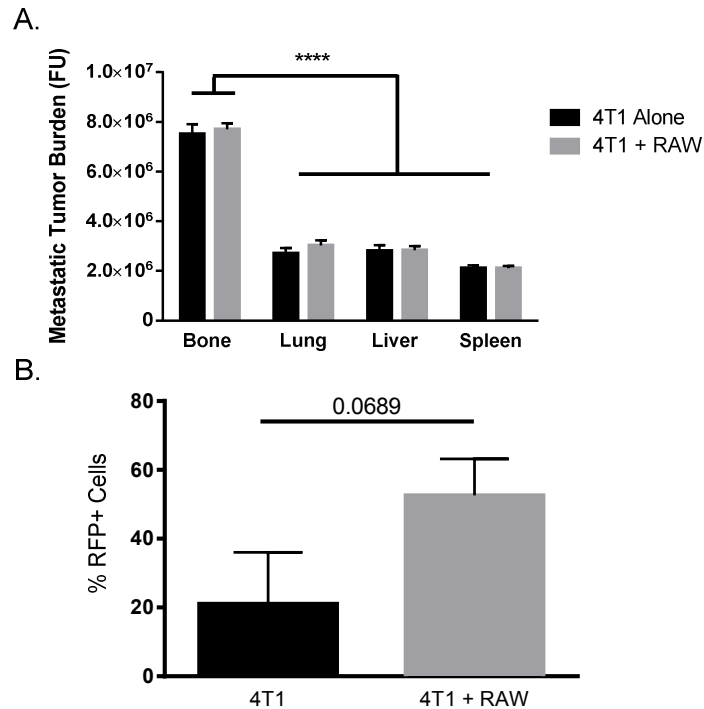


Figure 9. Metastatic burden of 4T1-RFP subcutaneous tumors in BALB/c mice. A. Bone metastatic burden is significantly increased regardless of tumor type compared to all other sites ($n=8$). B. Percent of RFP positive cells within the bone marrow of mice injected with either 4T1-RFP alone or in combination with RAW macrophages ($p=0.0689$, $n=4$). Data points are represented as the mean \pm SEM. **** $p < 0.0001$

7 – The hypoxic environment differentially affected 4T1-RFP cells growth in *in vitro* co-cultures of 4T1-RFP cells and RAW macrophages

To determine whether the RAW macrophages directly influence tumor cell proliferation, 4T1-RFP carcinoma cells and RAW macrophages (5:1 ratio) were co-cultured for 48 hours in normoxic ($\sim 21\% O_2$) and hypoxic ($< 1\% O_2$) conditions.

Following the incubation, growth of 4T1-RFP cells in co-culture was evaluated using

fluorescent microscopy in which the intensity of RFP per number of nuclei was determined (Figure 10).

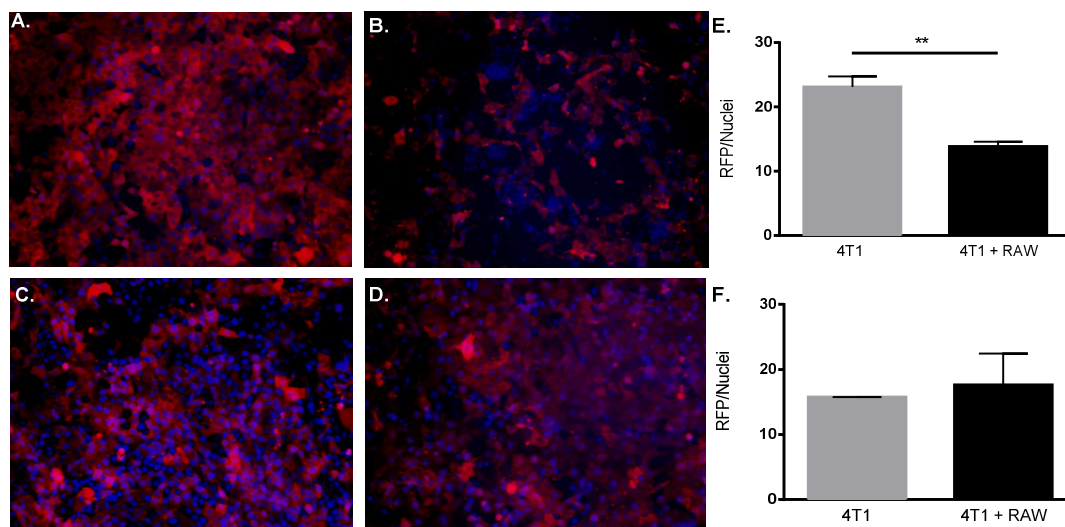


Figure 10. Growth of 4T1-RFP alone or in co-culture with RAW macrophages. Representative microphotographs of 4T1-RFP alone (left) or in co-culture with RAW (right) in normoxic (top row) and hypoxic (bottom row) conditions. Quantification of normoxic (E) and hypoxic (F) microphotographs using Cellprofiler software. Scale bar is 200 μm . ** $p < 0.01$.

The growth of the 4T1-RFP cells was further assessed by determining the intensity of the RFP and Hoechst fluorescence using a plate reader. In normoxic conditions, growth of 4T1-RFP cells was significantly slower than when co-cultured with RAW macrophages compared to 4T1-RFP cultured alone ($p = 0.0023$, $n = 4$, Figure 11A). In contrast, in hypoxic conditions, 4T1-RFP cells grew at a similar rate whether cultured alone or in the presence of RAW macrophages ($p = 0.7237$, $n = 2$, Figure 11B). These observations indicated that the hypoxic microenvironment either directly enhances the RAW macrophage pro-tumor signaling or indirectly influences the tumor cell function. To assess whether this observation is a feature of the RAW macrophages,

similar experiments were conducted with BMDMs. In contrast to the addition of RAW macrophages, co-culturing BMDMs with 4T1-RFP cells in the conditions tested either in normoxic ($p = 0.3543$) or hypoxic ($p = 0.1108$) environments, did not significantly alter 4T1-RFP cell growth ($n = 2$, Figure 12).

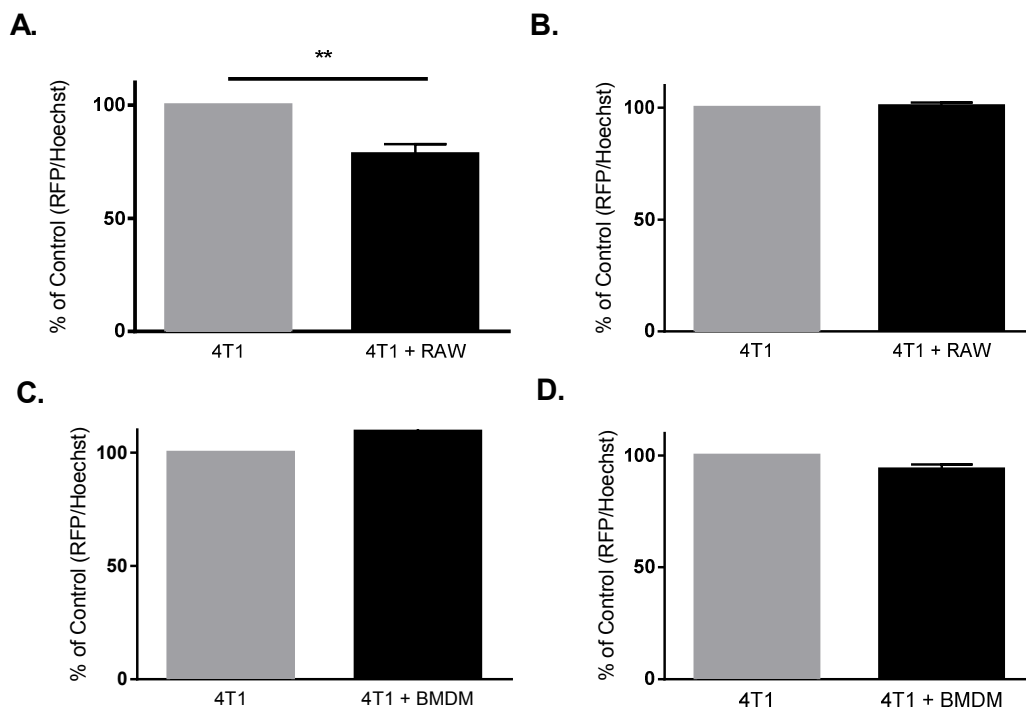


Figure 11. Growth of 4T1-RFP alone or in co-culture with RAW macrophages. There is a significant decrease in growth of 4T1-RFP when co-cultured with RAW in normoxic conditions ($n=4$). (B) There are no observed differences in the growth of 4T1-RFP when co-cultured with RAW in hypoxic conditions ($n = 2$). There is no change in the growth of 4T1-RFP when co-cultured with BMDM in either normoxic (C) or hypoxic (D)

CHAPTER FOUR: DISCUSSION

In the present study we investigated the effects of macrophages in mammary tumor progression and observed the following. (1) Co-implantation of 4T1-RFP and RAW cells significantly decreased primary tumor volume but tended to increase metastases to the bone marrow. (2) Furthermore, CD11b⁺ cell infiltration was higher in primary tumors derived from co-implantation of 4T1-RFP and RAW cells. (3) Interestingly, apoptosis but not hypoxia was markedly increased in primary tumors injected with 4T1-RFP alone. (4) Consistent with the *in vivo* observations, in normoxic conditions co-culturing 4T1-RFP and RAW cells led to a reduction in the growth of 4T1-RFP cells compared to 4T1-RFP cells cultured alone. However, in hypoxic conditions in similar co-cultures, 4T1-RFP cell growth was unaffected by the addition of RAW macrophages. (5) In contrast with co-cultures using RAW macrophages, regardless of oxygen conditions, the addition of BMDMs to 4T1-RFP cells does not alter the growth of 4T1-RFP cells. (6) Finally, differential NRP-1 expression was detected between RAW macrophages and BMDMs.

In vivo, co-implantation of 4T1 mammary carcinoma cells with M2 polarized BMDMs significantly enhanced primary tumor growth and metastases to the lungs [64]. Here, as macrophages retain plasticity after polarization [70, 71], RAW macrophages were not polarized *in vitro* prior to implantation. Indeed, post-implantation the phenotype of the co-injected macrophages is dependent on the new environmental stimuli they

encounter [50, 69]. Thus, the ability of co-implantation to significantly decrease primary tumor growth is likely dependent on the development of an anti-tumor microenvironment including M1-polarized macrophages. In preclinical models of lung, pancreatic and spontaneous mammary carcinoma, maintenance of a M1 macrophage phenotype can be achieved by decreasing macrophage expression of NRP-1, which impedes macrophage entry into hypoxic tumor areas [39]. Concurrently, when macrophages are prevented from entering hypoxic tumor areas, primary tumor growth and metastases are decreased while CD11b⁺ cells are increased [39]. Our observations confirm in an orthotopic breast cancer model these previous observations. Furthermore, our data highlight that decreases in primary tumor size are associated with enhanced ability of tumor cells from the co-implanted tumors to colonize the bones. Together, these observations underline the critical need to further our understanding of the role of macrophage subsets in cancer progression especially the promotion of metastases in light of ongoing clinical development of immunotherapy [72].

Although a significant increase in the CD11b positive cell population was observed in mammary tumors isolated from mice co-implanted with 4T1 and RAW cells, further characterization of this population is required. Particularly, RAW macrophages are an immune cell type, that like other host immune cells should express CD11b. CD11b is the alpha subunit of a heterodimeric cell surface integrin receptor that is primarily expressed on mature myeloid cells [73]. Primarily these cells include monocytes, macrophages, and granulocytes (most notably neutrophils) [67]. Therefore, determination of whether this significant increase in population is merely due to the co-injection of RAW cells, proliferation of the RAW (or a subset), or actual infiltration of host immune

CD11b positive cells is critical. Distinguishing host CD11b positive myeloid immune cells from the co-implanted RAW macrophages may be completed by fluorescent *in situ* hybridization of tumor sections, specifically probing for the portion of the Abelson murine leukemia virus which RAW macrophages integrated [74, 75] while concurrently, probing for CD11b expression [76]. Alternatively, compared to primary macrophages, RAW 264.7 macrophage expression of IL1 β has been shown to be significantly lower for example following challenges with LPS and subsequently with silica nanoparticles [77]. The alteration in ASC expression in RAW macrophage may lead to reduced IL1 β expression as pro-caspase 1 is not activated into caspase 1 preventing/limiting the secretion of active IL1 β and thereby local inflammation as shown in otitis [78]. Thus ASC and CD11b expression may also permit to evaluate the respective contributions of RAW co-implanted macrophages and native infiltrating macrophages in the 4T1 tumor reduced progression observed here.

Previously, CD11b⁺ cells have been demonstrated to be the predominant immune cell type infiltrating 4T1 primary tumors while lymphoid (CD3⁺) cells typically comprise less than five percent of the infiltrating immune cells (CD45⁺) [79]. Thus our data confirm previous observations in the 4T1 murine models [80]. In addition, infiltration by a high number of CD11b⁺ cells of the primary tumor mass along with a simultaneous decrease in tumor growth contrast with the enhanced bone metastases. As the CD11b⁺ population within 4T1 tumors is typically heterogeneous, differences in primary tumor and metastatic progression may be associated with variations within the local microenvironment of the tumor cells.

Apoptosis was markedly observed in primary tumors obtained from animals implanted with 4T1 cells alone differing with limited apoptosis detected in primary tumors collected from mice co-implanted with 4T1 and RAW cells. This observation contrasts with the expected increased apoptosis in 4T1 carcinoma cells leading to a reduced tumor volume that could be associated with a high CD11b positive cell infiltration. Alternatively, although tumor apoptosis is high in 4T1 generated tumors, cells may divide even faster, leading to a net growth of the tumor mass. Moreover, significant increases in caspase-3 expression are observed in patients with high grade ductal carcinoma *in situ* as compared to both low and intermediate grade disease [81]. Furthermore, mathematical modeling and computer simulations suggest that increasing apoptosis levels may limit tumor growth at first, but enhances tumor growth over time as more aggressive, apoptosis resistant tumor cells are selected [82]. Thus, the reduced caspase-3 expression in co-injected tumors is partly consistent with RAW macrophages preventing tumor progression possibly through inhibition of 4T1 cell proliferation. Accordingly, further work will evaluate proliferation markers (Ki67 and PCNA) along with apoptosis markers (e.g., active caspase 3) using IHC staining of the implanted tumors to determine the net growth, so as to more accurately describe the growth of the tumors in animals implanted with tumor alone or co-implanted with tumor and macrophages.

Moreover, our *in vitro* experiments demonstrated that co-culturing 4T1 and RAW macrophages in normoxia resulted in a significant decrease in the number of 4T1 cells suggesting that the RAW macrophages were capable of slowing tumor cell growth. In contrast, in hypoxic conditions the addition of RAW macrophages did not alter the

growth of 4T1-RFP cells. These observations are in line with recent evidence highlighting, within the tumor mass, the key importance of the hypoxic and normoxic zones in cancer progression [24, 39, 48, 56, 57]. This work also underlines the need to investigate the tumor microenvironment studying normoxic and hypoxic zones separately.

NRP-1 is responsible for homing macrophages to hypoxic regions of the tumor mass and thereby promoting tumor growth [39]. Our findings suggest that the mean fluorescence intensity of RAW cell NRP-1 expression tended to be lower than BMDMs and we concurrently observed differential effects of these two cell types on growth patterns of 4T1. Collectively, these findings suggest that indeed decreased expression of NRP-1 on the surface of RAW macrophages as compared to BMDM alters their functional response within the tumor microenvironment. Likely this is a result of a diminished ability of the RAW macrophages to localize to the hypoxic microenvironment thus preventing M2 polarization. However, further investigations are warranted as other differences between BMDMs and RAW macrophages could be responsible for the differential responses observed.

CHAPTER FIVE: CONCLUSION & PERSPECTIVES

Taken together our data highlight the key role of the microenvironment in breast tumor progression especially the importance of oxygen conditions and macrophage phenotype in promoting tumor progression and metastasis. Below, we point out aspects of the present research that warrant further investigations.

Most notably, the contrasting observations that 4T1 cells with RAW macrophages expressing low NRP-1 in vivo leads to a significant reduction in tumor size while simultaneously enhancing bone marrow metastases are interesting. The present data are the first to investigate the effects of macrophage NRP-1 expression in an orthotopic immunocompetent model of mammary tumor progression, and they confirm observations made in lung, spontaneous mammary and pancreatic cancer models [39]. Interestingly, enhanced bone metastasis despite reduced primary tumor size is a novel finding critical for the understanding of breast tumor progression toward metastasis. Future experiments will detail and further investigate the CD11b cellular subsets, their NRP-1 expression and their effects on primary tumor growth and the development of bone metastases.

Indeed, to further evaluate the mechanisms by which co-implantation of 4T1 cells with RAW macrophages differentially regulate tumor progression, the CD11b population needs to be additionally characterized. Given that CD11b expression is present on multiple myeloid cell types, identifying which subset of CD11b cells are present within the co-implanted tumors may assist in determining how the tumor microenvironment is

capable of both limiting primary tumor progression while enhancing bone metastases. Our previous work demonstrated a large infiltration of polymorphonuclear (PMN) cells (mostly neutrophils) in 4T1 tumor masses [80], and others have demonstrated CD11b populations to be predominately of the macrophage lineage [79]. Whether the CD11b population present within the tumors generated by the co-injection of RAW and 4T1 cells is primarily composed of PMN cells and/or macrophages remains to be defined. Concurrently, the respective direct contributions of these cells in primary tumor regression or promotion of bone metastases, respectively, require additional evaluations.

Also, previous work has demonstrated that TAMs not only enhance tumor cell metastases by indirect contact (angiogenesis, matrix remodeling, etc...) but also can directly interact with and lead tumor cells out of the primary tumor [83]. Moreover, under appropriate microenvironmental conditions, progression of bone metastases is enhanced through heightened association with osteoclasts, i.e., bone specific multi-nucleated giant cells [84, 85]. As macrophages can directly differentiate into osteoclasts [86], the enhanced bone metastases observed here may be attributed to recruitment of a CD11b⁺ macrophage lineage capable of colonizing bones. To investigate this hypothesis, primary tumors and metastatic bone lesions from tumors implanted with 4T1 cells alone or in combination with RAW cells, could be investigated for CD11b and F4/80, a marker expressed at high levels on the surface of macrophages and low levels on monocytes.

Additionally, the mechanisms by which NRP-1 low expressing RAW cells influence 4T1-RFP cell growth should be evaluated. Obviously, the effects of the co-VEGF receptor on enhancing micro-vascularization and thus decreasing hypoxic regions in tumors are under investigation. Moreover, as only RAW cells (expressing low NRP1)

but not BMDM cells (higher NRP-1 expression) led to decreased 4T1 tumor growth, the influence of NRP-1 expression on direct tumor growth warrant further investigation.

Primarily, whether the ability of macrophages to decrease 4T1 cell growth is dependent on physical interactions, the secretion or shedding of specific molecules, or a combination of both interactions should be determined. Moreover, the specific effects of hypoxia on RAW and BMDM cells should be comparatively evaluated both in vitro and in vivo so as to further elucidate the mechanisms underlying their differential effects on breast cancer progression.

REFERENCES

1. Siegel, R.L., K.D. Miller, and A. Jemal, *Cancer statistics, 2015*. CA Cancer J Clin, 2015.
2. NCCN., N., *NCCN Clinical Practice Guidelines in Oncology*. 2014. Version 3.2014.
3. Bissell, M.J. and W.C. Hines, *Why don't we get more cancer? A proposed role of the microenvironment in restraining cancer progression*. Nat Med, 2011. 17(3): p. 320-9.
4. Gangadhara, S., et al., *Pro-metastatic tumor-stroma interactions in breast cancer*. Future Oncol, 2012. 8(11): p. 1427-42.
5. Mao, Y., et al., *Stromal cells in tumor microenvironment and breast cancer*. Cancer Metastasis Rev, 2013. 32(1-2): p. 303-15.
6. Rohan, T.E., et al., *Tumor microenvironment of metastasis and risk of distant metastasis of breast cancer*. J Natl Cancer Inst, 2014. 106(8).
7. Folkman, J., *Tumor angiogenesis: therapeutic implications*. N Engl J Med, 1971. 285(21): p. 1182-6.
8. Kitamura, T., B.Z. Qian, and J.W. Pollard, *Immune cell promotion of metastasis*. Nat Rev Immunol, 2015. 15(2): p. 73-86.
9. Schneider, B.P. and K.D. Miller, *Angiogenesis of breast cancer*. J Clin Oncol, 2005. 23(8): p. 1782-90.
10. Sonnenschein, C. and A.M. Soto, *The aging of the 2000 and 2011 Hallmarks of Cancer reviews: a critique*. J Biosci, 2013. 38(3): p. 651-63.
11. Bizzarri, M. and A. Cucina, *Tumor and the microenvironment: a chance to reframe the paradigm of carcinogenesis?* Biomed Res Int, 2014. 2014: p. 934038.
12. Nielsen, M., et al., *Breast cancer and atypia among young and middle-aged women: a study of 110 medicolegal autopsies*. Br J Cancer, 1987. 56(6): p. 814-9.
13. Booth, B.W., et al., *The normal mammary microenvironment suppresses the tumorigenic phenotype of mouse mammary tumor virus-neu-transformed mammary tumor cells*. Oncogene, 2011. 30(6): p. 679-89.
14. Bussard, K.M., et al., *Reprogramming human cancer cells in the mouse mammary gland*. Cancer Res, 2010. 70(15): p. 6336-43.
15. Martin, L.J. and N.F. Boyd, *Mammographic density. Potential mechanisms of breast cancer risk associated with mammographic density: hypotheses based on epidemiological evidence*. Breast Cancer Res, 2008. 10(1): p. 201.

16. Sternlicht, M.D., et al., *The stromal proteinase MMP3/stromelysin-1 promotes mammary carcinogenesis*. Cell, 1999. 98(2): p. 137-46.
17. Maffini, M.V., et al., *The stroma as a crucial target in rat mammary gland carcinogenesis*. J Cell Sci, 2004. 117(Pt 8): p. 1495-502.
18. Bao, L., et al., *Effects of inoculation site and Matrigel on growth and metastasis of human breast cancer cells*. Br J Cancer, 1994. 70(2): p. 228-32.
19. Fridman, R., et al., *Increased initiation and growth of tumor cell lines, cancer stem cells and biopsy material in mice using basement membrane matrix protein (Cultrex or Matrigel) co-injection*. Nat Protoc, 2012. 7(6): p. 1138-44.
20. DeNardo, D.G. and L.M. Coussens, *Inflammation and breast cancer. Balancing immune response: crosstalk between adaptive and innate immune cells during breast cancer progression*. Breast Cancer Res, 2007. 9(4): p. 212.
21. Toi, M., et al., *Tumor angiogenesis in breast cancer: its importance as a prognostic indicator and the association with vascular endothelial growth factor expression*. Breast Cancer Res Treat, 1995. 36(2): p. 193-204.
22. Weidner, N., et al., *Tumor angiogenesis and metastasis--correlation in invasive breast carcinoma*. N Engl J Med, 1991. 324(1): p. 1-8.
23. Kim, Y., et al., *Hypoxic tumor microenvironment and cancer cell differentiation*. Curr Mol Med, 2009. 9(4): p. 425-34.
24. Bos, R., et al., *Levels of hypoxia-inducible factor-1 alpha during breast carcinogenesis*. J Natl Cancer Inst, 2001. 93(4): p. 309-14.
25. Ziello, J.E., I.S. Jovin, and Y. Huang, *Hypoxia-Inducible Factor (HIF)-1 regulatory pathway and its potential for therapeutic intervention in malignancy and ischemia*. Yale J Biol Med, 2007. 80(2): p. 51-60.
26. Ke, Q. and M. Costa, *Hypoxia-inducible factor-1 (HIF-1)*. Mol Pharmacol, 2006. 70(5): p. 1469-80.
27. Fox, S.B., D.G. Generali, and A.L. Harris, *Breast tumour angiogenesis*. Breast Cancer Res, 2007. 9(6): p. 216.
28. Hoeben, A., et al., *Vascular endothelial growth factor and angiogenesis*. Pharmacol Rev, 2004. 56(4): p. 549-80.
29. Zachary, I.C., *How neuropilin-1 regulates receptor tyrosine kinase signalling: the knowns and known unknowns*. Biochem Soc Trans, 2011. 39(6): p. 1583-91.

30. Djordjevic, S. and P.C. Driscoll, *Targeting VEGF signalling via the neuropilin co-receptor*. Drug Discov Today, 2013. 18(9-10): p. 447-55.
31. Herzog, B., et al., *VEGF binding to NRP1 is essential for VEGF stimulation of endothelial cell migration, complex formation between NRP1 and VEGFR2, and signaling via FAK Tyr407 phosphorylation*. Mol Biol Cell, 2011. 22(15): p. 2766-76.
32. Meyer, R.D., M. Mohammadi, and N. Rahimi, *A single amino acid substitution in the activation loop defines the decoy characteristic of VEGFR-1/FLT-1*. J Biol Chem, 2006. 281(2): p. 867-75.
33. Yazdani, U. and J.R. Terman, *The semaphorins*. Genome Biol, 2006. 7(3): p. 211.
34. Takamatsu, H. and A. Kumanogoh, *Diverse roles for semaphorin-plexin signaling in the immune system*. Trends Immunol, 2012. 33(3): p. 127-35.
35. Worzfeld, T. and S. Offermanns, *Semaphorins and plexins as therapeutic targets*. Nat Rev Drug Discov, 2014. 13(8): p. 603-21.
36. Kumanogoh, A. and H. Kikutani, *Immunological functions of the neuropilins and plexins as receptors for semaphorins*. Nat Rev Immunol, 2013. 13(11): p. 802-14.
37. Dejda, A., et al., *Neuropilin-1 mediates myeloid cell chemoattraction and influences retinal neuroimmune crosstalk*. J Clin Invest, 2014. 124(11): p. 4807-22.
38. Takamatsu, H., et al., *Semaphorins guide the entry of dendritic cells into the lymphatics by activating myosin II*. Nat Immunol, 2010. 11(7): p. 594-600.
39. Casazza, A., et al., *Impeding macrophage entry into hypoxic tumor areas by *Sema3A/Nrp1* signaling blockade inhibits angiogenesis and restores antitumor immunity*. Cancer Cell, 2013. 24(6): p. 695-709.
40. Plein, A., A. Fantin, and C. Ruhrberg, *Neuropilin regulation of angiogenesis, arteriogenesis, and vascular permeability*. Microcirculation, 2014. 21(4): p. 315-23.
41. Ellis, L.M., *The role of neuropilins in cancer*. Mol Cancer Ther, 2006. 5(5): p. 1099-107.
42. Soker, S., et al., *Neuropilin-1 is expressed by endothelial and tumor cells as an isoform-specific receptor for vascular endothelial growth factor*. Cell, 1998. 92(6): p. 735-45.
43. Miao, H.Q., et al., *Neuropilin-1 expression by tumor cells promotes tumor angiogenesis and progression*. FASEB J, 2000. 14(15): p. 2532-9.
44. Dunn, G.P., L.J. Old, and R.D. Schreiber, *The immunobiology of cancer immunosurveillance and immunoediting*. Immunity, 2004. 21(2): p. 137-48.

45. Schroder, K., et al., *Interferon-gamma: an overview of signals, mechanisms and functions*. J Leukoc Biol, 2004. 75(2): p. 163-89.
46. Töpfer, K., et al., *Tumor Evasion from T Cell Surveillance*. J Biomed Biotechnol, 2011. 2011.
47. Staveley-O'Carroll, K., et al., *Induction of antigen-specific T cell anergy: An early event in the course of tumor progression*. Proc Natl Acad Sci U S A, 1998. 95(3): p. 1178-83.
48. Hao, N.B., et al., *Macrophages in tumor microenvironments and the progression of tumors*. Clin Dev Immunol, 2012. 2012: p. 948098.
49. Sica, A., et al., *Macrophage polarization in tumour progression*. Semin Cancer Biol, 2008. 18(5): p. 349-55.
50. Mantovani, A. and M. Locati, *Tumor-associated macrophages as a paradigm of macrophage plasticity, diversity, and polarization: lessons and open questions*. Arterioscler Thromb Vasc Biol, 2013. 33(7): p. 1478-83.
51. Solinas, G., et al., *Tumor-associated macrophages (TAM) as major players of the cancer-related inflammation*. J Leukoc Biol, 2009. 86(5): p. 1065-73.
52. Lewis, C.E. and J.W. Pollard, *Distinct role of macrophages in different tumor microenvironments*. Cancer Res, 2006. 66(2): p. 605-12.
53. Schmierer, A., et al., *Differentiation and gene expression profile of tumor-associated macrophages*. Semin Cancer Biol, 2012. 22(4): p. 289-97.
54. Zhang, M., et al., *A high M1/M2 ratio of tumor-associated macrophages is associated with extended survival in ovarian cancer patients*. J Ovarian Res, 2014. 7: p. 19.
55. Escribese, M.M., M. Casas, and A.L. Corbi, *Influence of low oxygen tensions on macrophage polarization*. Immunobiology, 2012. 217(12): p. 1233-40.
56. Riboldi, E., et al., *Hypoxia-mediated regulation of macrophage functions in pathophysiology*. Int Immunol, 2013. 25(2): p. 67-75.
57. Tripathi, C., et al., *Macrophages are recruited to hypoxic tumor areas and acquire a pro-angiogenic M2-polarized phenotype via hypoxic cancer cell derived cytokines Oncostatin M and Eotaxin*. Oncotarget, 2014. 5(14): p. 5350-68.
58. Dace, D.S., et al., *Interleukin-10 promotes pathological angiogenesis by regulating macrophage response to hypoxia during development*. PLoS One, 2008. 3(10): p. e3381.
59. Jarnicki, A.G., et al., *Suppression of antitumor immunity by IL-10 and TGF-beta-producing T cells infiltrating the growing tumor: influence of tumor environment on the induction of CD4+ and CD8+ regulatory T cells*. J Immunol, 2006. 177(2): p. 896-904.

60. Wu, W.K., et al., *IL-10 regulation of macrophage VEGF production is dependent on macrophage polarisation and hypoxia*. Immunobiology, 2010. 215(9-10): p. 796-803.
61. Jeon, S.H., et al., *Mechanisms underlying TGF-beta1-induced expression of VEGF and Flk-1 in mouse macrophages and their implications for angiogenesis*. J Leukoc Biol, 2007. 81(2): p. 557-66.
62. Rego, S.L., R.S. Helms, and D. Dreau, *Breast tumor cell TACE-shed MCSF promotes pro-angiogenic macrophages through NF-kappaB signaling*. Angiogenesis, 2014. 17(3): p. 573-85.
63. Rego, S.L., R.S. Helms, and D. Dreau, *Tumor necrosis factor-alpha-converting enzyme activities and tumor-associated macrophages in breast cancer*. Immunol Res, 2014. 58(1): p. 87-100.
64. Cho, H.J., et al., *Bone marrow-derived, alternatively activated macrophages enhance solid tumor growth and lung metastasis of mammary carcinoma cells in a Balb/C mouse orthotopic model*. Breast Cancer Res, 2012. 14(3): p. R81.
65. Zhang, X., R. Goncalves, and D.M. Mosser, *The Isolation and Characterization of Murine Macrophages*. Curr Protoc Immunol, 2008. CHAPTER: p. Unit-14 1.
66. Feldman JP, G.R., *Quantitative Methods Inquires: A mathematical model for tumor volume evaluation*. . Methods. 4(4): p. 455-462.
67. Dziennis, S., et al., *The CD11b promoter directs high-level expression of reporter genes in macrophages in transgenic mice*. Blood, 1995. 85(2): p. 319-29.
68. Nicholson, D.W., et al., *Identification and inhibition of the ICE/CED-3 protease necessary for mammalian apoptosis*. Nature, 1995. 376(6535): p. 37-43.
69. Mantovani, A. and A. Sica, *Macrophages, innate immunity and cancer: balance, tolerance, and diversity*. Curr Opin Immunol, 2010. 22(2): p. 231-7.
70. Liu, H., et al., *In vitro repolarized tumor macrophages inhibit gastric tumor growth*. Oncol Res, 2013. 20(7): p. 275-80.
71. Davis, M.J., et al., *Macrophage M1/M2 polarization dynamically adapts to changes in cytokine microenvironments in Cryptococcus neoformans infection*. MBio, 2013. 4(3): p. e00264-13.
72. Fridlender, Z.G., et al., *Using macrophage activation to augment immunotherapy of established tumours*. Br J Cancer, 2013. 108(6): p. 1288-97.
73. Pahl, H.L., A.G. Rosmarin, and D.G. Tenen, *Characterization of the myeloid-specific CD11b promoter*. Blood, 1992. 79(4): p. 865-70.

74. Baltimore, D., et al., *Structure and expression of the Abelson murine leukemia virus genome and its relationship to a normal cell gene*. Cold Spring Harb Symp Quant Biol, 1980. 44 Pt 2: p. 849-54.
75. Shields, A., et al., *Structure of the Abelson murine leukemia virus genome*. Cell, 1979. 18(4): p. 955-62.
76. Sholl, L.M., et al., *Combined use of ALK immunohistochemistry and FISH for optimal detection of ALK-rearranged lung adenocarcinomas*. J Thorac Oncol, 2013. 8(3): p. 322-8.
77. Sandberg, W.J., et al., *Comparison of non-crystalline silica nanoparticles in IL-1beta release from macrophages*. Part Fibre Toxicol, 2012. 9: p. 32.
78. Kurabi, A., et al., *The inflammasome adaptor ASC contributes to multiple innate immune processes in the resolution of otitis media*. Innate Immun, 2015. 21(2): p. 203-14.
79. DuPre, S.A., D. Redelman, and K.W. Hunter, Jr., *The mouse mammary carcinoma 4T1: characterization of the cellular landscape of primary tumours and metastatic tumour foci*. Int J Exp Pathol, 2007. 88(5): p. 351-60.
80. Jewell, A.N., et al., *The endothelin axis stimulates the expression of pro-inflammatory cytokines and pro-migratory molecules in breast cancer*. Cancer Invest, 2010. 28(9): p. 932-43.
81. Vakkala, M., P. Paakko, and Y. Soini, *Expression of caspases 3, 6 and 8 is increased in parallel with apoptosis and histological aggressiveness of the breast lesion*. Br J Cancer, 1999. 81(4): p. 592-9.
82. Enderling, H. and P. Hahnfeldt, *Cancer stem cells in solid tumors: is 'evading apoptosis' a hallmark of cancer?* Prog Biophys Mol Biol, 2011. 106(2): p. 391-9.
83. Condeelis, J. and J.W. Pollard, *Macrophages: obligate partners for tumor cell migration, invasion, and metastasis*. Cell, 2006. 124(2): p. 263-6.
84. Mizutani, K., et al., *The chemokine CCL2 increases prostate tumor growth and bone metastasis through macrophage and osteoclast recruitment*. Neoplasia, 2009. 11(11): p. 1235-42.
85. Vasiliadou I, a.H.I., *The role of macrophages in bone metastasis*. Journal of Bone Oncology, 2013. 2(4): p. 158-166.
86. Endo-Munoz, L., A. Evdokiou, and N.A. Saunders, *The role of osteoclasts and tumour-associated macrophages in osteosarcoma metastasis*. Biochim Biophys Acta, 2012. 1826(2): p. 434-42.